# 12% Efficiency CuIn(Se,S)2 Photovoltaic Device Prepared Using a Hydrazine Solution Process†

**ARTICLE** *in* CHEMISTRY OF MATERIALS · AUGUST 2009

Impact Factor: 8.35 · DOI: 10.1021/cm901950q



**6 AUTHORS**, INCLUDING:

Wei Liu

**8** PUBLICATIONS **509** CITATIONS

SEE PROFILE

Andrew J. Kellock

IBM

**106** PUBLICATIONS **3,198** CITATIONS

SEE PROFILE

CHEMISTRY OF MATERIALS
Article

*Chem. Mater.* **XXXX,** *XXX,* 000–000 A
DOI:10.1021/cm901950q

# 12% Efficiency $CuIn(Se,S)_2$ Photovoltaic Device Prepared Using a Hydrazine Solution Process†

Wei Liu,*,† David B. Mitzi,† Min Yuan,† Andrew J. Kellock,‡ S. Jay Chey,† and Oki Gunawan†

†*IBM T. J. Watson Research Center, P.O. Box 218, Yorktown Heights, New York 10598, and* ‡*IBM Almaden Research Center, 650 Harry Road, San Jose, California 95120.* †*Accepted as part of the 2010 "Materials Chemistry of Energy Conversion Special Issue".*

*Received July 1, 2009. Revised Manuscript Received August 12, 2009*

Thin-film $CuIn(Se,S)_2$ (i.e., CIS) absorbers have been solution-deposited using a hydrazine-based approach that offers the potential to significantly lower the fabrication cost for CIS solar cells. In this method, metal chalcogenides are completely dissolved in hydrazine, forming a homogeneous precursor solution. Film deposition is demonstrated by spin-coating of the precursor solution onto various substrates, including Mo-coated glass and thermally oxidized silicon wafers. Using this approach, no postdeposition anneal in a toxic Se or S-containing environment is needed to obtain CIS films. Instead, only a simple heat-treatment in an inert atmosphere is required, resulting in CIS films with good crystallinity. Bandgap tuning can readily be achieved by varying the amount of S incorporated into the film. Complete CIS devices with glass/Mo/CIS/CdS/i-ZnO/ITO structure are fabricated using absorbers produced via this hydrazine-based approach. Air Mass 1.5G power conversion efficiencies of as high as 12.2% have been achieved, demonstrating that this new approach has great potential as a low-cost alternative for high-efficiency CIS solar cell production.



## Introduction

With constant increase in worldwide energy demand and rising concerns regarding environmental pollution and global warming, clean renewable energy is beginning to be seen as the ultimate solution for addressing our future energy needs. Among all renewable energies, solar power is extremely promising as an abundant, clean energy source. However, photovoltaic technology is not widely deployed and solar energy does not yet constitute a significant percentage of everyday energy consumption ($\ll 1\%$ of total energy supply in 2007) due to the current high cost of solar panels. Currently, the photovoltaic (PV) market is dominated by crystalline Si-based technology. However for Si, an indirect bandgap material with low absorption coefficient, a thick (on the order of 100 $\mu$m) layer is generally required to efficiently absorb the photons in the solar spectrum. To reduce recombination within the thick layer, high-purity wafer-quality Si is therefore needed for traditional Si-based PV technology. In addition, Si technology relies on high-temperature vacuum-based processes during fabrication. Expensive equipment and complicated procedures make it even harder to reduce the final module cost. In contrast, polycrystalline thin-film $CuInSe_2$, $CuInS_2$ (CIS) and the alloy $CuIn_{1-x}Ga_xSe_2$ (CIGS) are direct bandgap materials. These chalcopyrites have much higher absorption coefficients and only require very thin layers (1−2 $\mu$m) to absorb a significant fraction of the incident solar radiation. In addition, CIS/CIGS offers high efficiency, long-term stability, and potential for low cost processing. Efficiencies of as high as 19.9% have been reported for lab-scale CIGS devices[1] (∼14% for CIS-based devices[2,3]). But these lab-scale high-quality absorbers are mostly deposited using expensive vacuum-based methods such as evaporation[1−3] and sputtering.[4,5] Sophisticated vacuum-based tools and control systems require large capital investment, thereby hindering the emerging CIS-based technologies from achieving profitable operation.

To address the cost issues that limit the CIS industry, efforts have been made to take an alternative approach to depositing CIS material. Reports of nonvacuum, solution-based approaches include a nanoparticle solution-based technique,[6,7] electrochemical deposition,[8,9] and

*Corresponding author. E-mail: wliu70@gmail.com; phone: 1-914-945-1797; fax: 1-914-945-4252.

(1) Repins, I.; Contreras, M. A.; Egaas, B.; DeHart, C.; Scharf, J.; Perkins, C. L.; To, B.; Noufi, R. *Prog. Photovoltaics* **2008**, *16*, 235.
(2) Stolt, L.; Hedström, J.; Kessler, J.; Ruckh, M.; Velthaus, K. O.; Schock, H. W. *Appl. Phys. Lett.* **1993**, *62*, 597.
(3) AbuShama, J.; Johnston, S.; Moriarty, T.; Teeter, G.; Ramanathan, K.; Noufi, R. *Prog. Photovoltaics* **2004**, *12*, 39.
(4) da Cunha, A. F.; Kurdzesau, F.; Salomé, P. M. P. *Mater. Sci. Forum* **2006**, *514−516*, 93.
(5) Hollars, D. R.; Dorn, R.; Paulson, P. D.; Titus, J.; Zubeck, R. *Mater. Res. Soc. Symp. Proc.* **2005**, *865*, F14.34.1.
(6) Kapur, V. K.; Bansal, A.; Le, P.; Asensio, O. I. *Thin Solid Films* **2003**, *431−432*, 53.
(7) Kaelin, M.; Rudmann, D.; Kurdesau, F.; Meyer, T.; Zogg, H.; Tiwari, A. N. *Thin Solid Films* **2003**, *431−432*, 58.
(8) Calixto, M. E.; Dobson, K. D.; McCandless, B. E.; Birkmire, R. W. In *Proceedings of the 31st IEEE Photovoltaic Specialist Conference*; Lake Buena Vista, FL, Jan 3−7, 2005; IEEE: Piscataway, NJ, 2005; p 378.
(9) Guimard, D.; Grand, P. P.; Bodereau, N.; Cowache, P.; Guillemoles, J. F.; Lincot, D.; Taunier, S.; Ben Farah, M.; Mogensen, P. In *Proceedings of the 29th IEEE Photovoltaic Specialist Conference*; New Orleans, LA, May 19−24, 2002; IEEE: Piscataway, NJ, 2002; p 692.

spray pyrolysis.[10−12] However, there are various limitations for these nonvacuum techniques. For example, the incorporation of undesired impurities, such as carbon, oxygen, and chlorine, from the precursor or solvent is almost universal for these solution-based technologies. The impurities can compromise device performance and are generally extremely difficult to be taken out of the CIS system.[13] Another issue for most currently reported solution-based techniques is the difficulty of incorporating Se into the system. A high temperature selenization process in, for example, a highly toxic $H_2Se$ environment, is therefore required for these solution-based techniques, sometimes in combination with a high temperature reduction step. Other issues, such as the complication of making precursor solutions, low throughput, and low material utilization often present barriers to making these techniques a real "low-cost", competitive solution for the current CIS PV industry.

Targeting the issues facing the current vacuum or solution-based CIS technology, we hereby present a potentially low-cost, clean, simple nonvacuum technique to deposit high quality $CuInSe_xS_{2-x}$ absorbers. This hydrazine-based technique involves three simple steps performed under an inert atmosphere to produce high quality CIS thin films: (1) dissolve constitutional elements in anhydrous hydrazine at room temperature; (2) deposit the precursor film on substrates, such as Mo coated soda-lime glass; (3) apply a heat treatment to the substrate to form the CIS absorber layer. By mixing appropriate amounts of chalcogenides with a selected amount of chalcogen and dissolving them in hydrazine, a stable clear solution is formed with stirring. In the solution, chalcogenide anions are separated by small hydrazinium ($N_2H_5^+$) cations and the elements are uniformly mixed on a molecular scale. Another advantage of the hydrazine precursor approach is that no undesired impurities such as C, O, Cl are introduced into the solution. Only the required elements (e.g., Cu, In, Se, S) are dissolved in the hydrazine solvent. Upon heating, the small, weakly coordinating hydrazine species readily leave the system without affecting film properties or leaving behind deleterious impurities. This method of preparing CIS precursor solutions and films is similar to that described previously for making solution-processed chalcogenide-based thin-film transistors[14−16] and is also analogous to that recently reported for preparing solution-deposited $CuIn_{1-x}Ga_xSe_2$ solar cells, with $x \approx 0.3$.[17−19] In the current report, we extend these solar cell results to the non-Ga-containing ($x \approx 0$) end member. Using this hydrazine-based approach, CIS absorbers were successfully deposited and, instead of adding Ga to adjust the bandgap, the amount of S in the film was varied to tune the bandgap of the system. As a result, device efficiency has been improved compared to earlier reported results[20,21] to 12.2%—a value that is on par with the record values for vacuum-deposited $CuInS_2$ (11.4%[22] or 12.2% calculated using quantum efficiency data[23]) and $CuIn(Se,S)_2$ (~10%[24]) devices. Although the currently reported value is slightly lower than the record ~14% efficiency obtained using lower bandgap $CuInSe_2$ deposited via the three-stage vacuum evaporation process,[3] the higher voltage obtained by adding S is more desirable for module applications.

## Experimental Section

**Solution Preparation.** All experiments were done in a nitrogen drybox system to ensure an inert atmosphere (oxygen and water levels maintained below 1 ppm). Cu and In source solutions were individually prepared and then mixed together with different ratios to adjust the Cu to In ratio. The solvent used was anhydrous hydrazine (Aldrich, 98%). ***Caution!*** *Hydrazine is highly toxic and should be handled using appropriate protective equipment to prevent contact with either the vapors or liquid.*

To prepare the Cu precursor solution, we dissolved 6 mmol of $Cu_2S$ (0.955 g) and 12 mmol of S (0.385 g) in 12 mL of hydrazine, which produced a clear yellow solution after stirring for a few days. Two types of In precursor solutions have been prepared. Type one was prepared by dissolving 3 mmol of $In_2Se_3$ (1.399 g) and 3 mmol of Se (0.237 g) in 12 mL of hydrazine, which will be noted as "$In_2Se_3$ precursor" in this paper. After being stirred for a few days, the $In_2Se_3$ precursor turned into a clear colorless solution with some viscosity. To increase the S content in the final film, we prepared another type of In precursor by using the same molar amount of sulfur to replace the Se used for preparing the $In_2Se_3$ precursor. Three millimoles of $In_2Se_3$ (1.399 g) and 3 mmol of S (0.096 g) were dissolved in 12 mL of hydrazine, producing a colorless and more viscous solution than the $In_2Se_3$ precursor. This solution will be noted as "$In_2(Se,S)_3$ precursor". In addition, separate chalcogen solutions were prepared to controllably introduce extra chalcogen and also adjust the Se to S ratio. For example, a darkly colored Se solution was prepared by dissolving 4 mmol Se (0.316 g) in 2.0 mL of hydrazine and a colorless S solution was prepared by dissolving 4 mmol S (0.128 g) in 2.0 mL hydrazine.

The final spin-coating solution was prepared by mixing the above-mentioned solutions in the appropriate volumes to yield the desired Cu:In ratio. For example, to target a $Cu_{0.8}InSe_{2-x}S_x$

(10) Krunks, M.; Mikli, V.; Bijakina, O.; Mellikov, E. *Appl. Surf. Sci.* **1999**, *142*, 356.
(11) Jin, M. H.; Banger, K. K.; Harris, J. D.; Cowen, J. E.; Hepp, A. F. In *Proceedings of the 29th IEEE Photovoltaic Specialist Conference*; New Orleans, LA, May 19−24, 2002; p 672.
(12) Shirakata, S.; Terasako, T.; Kariya, T. *J. Phys. Chem. Solids* **2005**, *66*, 1970.
(13) Kaelin, M.; Zogg, H.; Tiwari, A. N.; Wilhelm, O.; Pratsinis, S. E.; Meyer, T.; Meyer, A. *Thin Solid Films* **2004**, *457*, 391.
(14) Mitzi, D. B.; Kosbar, L. L.; Murray, C. E.; Copel, M.; Afzali, A. *Nature* **2004**, *428*, 299.
(15) Mitzi, D. B.; Copel, M.; Murray, C. E. *Adv. Mater.* **2006**, *18*, 2448.
(16) Milliron, D. J.; Mitzi, D. B.; Copel, M.; Murray, C. E. *Chem. Mater.* **2006**, *18*, 587.
(17) Mitzi, D. B.; Yuan, M.; Liu, W.; Kellock, A. J.; Chey, S. J.; Deline, V.; Schrott, A. G. *Adv. Mater.* **2008**, *20*, 3657.
(18) Mitzi, D. B.; Yuan, M.; Liu, W.; Kellock, A. J.; Chey, S. J.; Gignac, L.; Schrott, A. G. *Thin Solid Films* **2009**, *517*, 2158.
(19) Mitzi, D. B.; Yuan, M.; Liu, W.; Kellock, A. J.; Chey, S. J., Schrott, A. G.; Deline V. In *Proceedings of the 33rd IEEE Photovoltaic Specialist Conference*; San Diego, CA, May 11−16, 2008; IEEE: Piscataway, NJ, 2008; p384.
(20) Liu, W.; Mitzi, D. B.; Chey, S. J.; Kellock, A. *Mater. Res. Soc. Symp. Proc.* **2009**, *1123*, P06−03/F07−03.
(21) Hou, W. W.; Li, S.; Tung, C.; Kaner, R. B.; Yang, Y. In *Solar Energy: New Materials and Nanostructured Devices for High Efficiency*; Optical Society of America: Washington, D.C., 2008; paper SWC1.
(22) Siemer, K.; Klaer, J.; Luck, I.; Bruns, J.; Klenk, R.; Bräunig, D. *Sol. Energy Mater. Sol. Cells* **2001**, *67*, 159.
(23) Braunger, D.; Dürr, Th.; Hariskos, D.; Köble, Ch.; Walter, Th.; Wieser, N.; Schock, H. W. *25th IEEE Photovoltaic Specialists Conference*; IEEE: Piscataway, NJ, 1996; p 1001.
(24) Alberts, V.; Dejene, F. D. *J. Phys. D: Appl. Phys.* **2002**, *35*, 2021.

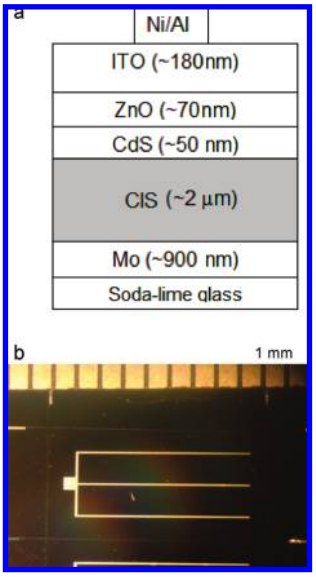


**Figure 1.** (a) Schematic image of the cross-section of a CIS device structure with approximate layer thickness. (b) Top view of a completed CIS device taken with a ruler showing the dimension. Each mark is 1 mm in length.



stoichiometry with minimum amount of S incorporated in the film, 0.64 mL Cu solution (0.64 mmol Cu) was mixed with 1.6 mL o f$In_2Se_3$ solution (0.8 mmol In and 1.6 mmol Se), 0.2 mL o fSe solution (0.4 mmol Se) and 0.36 mL of anhydrous hydrazine. An extra amount of Se was added to the solution to compensate the loss of chalcogen during the heating process and to also affect the Se to S ratio in the final film. For consistent solution concentration, extra hydrazine was added to make the final solution contain 0.29 mmol In (or CIS) per mL of solution. To produce a final film with more S incorporated, we prepared a similar solution and the $In_2(Se,S)_3$ precursor was used as the indium source, introducing more S into the system. The final precursor solutions were stirred for at least 1 h before deposition.

**Thin Film Deposition and Device Fabrication.** Thin films were deposited using spin coating on Mo-coated soda-lime glass substrates. The precursor solution was passed through a 0.2 $\mu$m PTFE filter and then flooded onto the substrate. Spin-coating was done at 800 rpm for 90 s. To achieve films with 1−2.5 $\mu$m thickness, multiple spin-coatings were used (~200−300 nm per layer). In between depositions, the substrate was placed on a preheated hot plate at ~300 °C for 5 min to dry and partially decompose the film. This heat treatment prevents the film from being redissolved during the next spin-coating operation. After all depositions were finished, a final high-temperature annealing was implemented to drive away any residual hydrazine and extra chalcogen species and to allow grain growth within the CIS thin films.

All PV devices adopted the substrate structure as shown in Figure 1a. CIS thin films were deposited on 2.54 × 2.54 $cm^2$ soda-lime glass pieces (0.1 cm thickness) coated with approximately 900 nm sputtered Mo. For device purposes, multiple layers of CIS films were spin-coated using the process described above to achieve a thickness of between 1.5 and 2.5 $\mu$m (as measured via SEM cross section analysis). Final annealing was done at approximately 500−550 °C for a period of 5−20 min. The n-type junction partner CdS (approximately 50 nm thick) was deposited using a chemical bath deposition, similar to what was described previously.[25] The CdS side of the substrate was then sputter coated with an approximately 70 nm thick layer of

(25) Contreras, M. A.; Romero, M. J.; To, B.; Hasoon, F.; Noufi, R.; Ward, S.; Ramanathan, K. *Thin Solid Films* **2002**, *403*−*404*, 204.

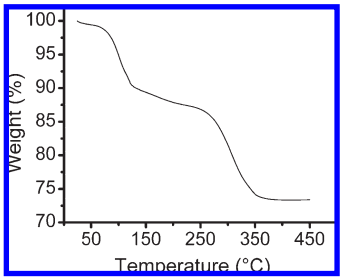


**Figure 2.** TGA data of a CIS precursor (1 °C/min ramp; $N_2$ atmosphere).

intrinsic ZnO followed by 180 nm of transparent conductive indium tin oxide. The optical transmission of the ITO layer was maintained above 80% in the visible spectral range while the sheet resistance was approximately 20 to 50 Ω/□. A Ni (50 nm)/Al (3 $\mu$m) dual layer top contact grid was evaporated through a metal mask to finish the device. Ni acts as an inert layer to prevent Al from being oxidized through contacting with ITO. Finally, a $MgF_2$ antireflection layer of approximately 100 nm was evaporated on top of the device to further increase the photogenerated current. The device total area (~0.45 $cm^2$) was defined by isolating the multilayer film from adjacent areas via mechanical scribing down to the Mo back contract layer. Figure 1b shows the top view of a finished device.

**Characterization.** Thermogravimetric analysis (TGA) was performed on a TA Instruments TGA-2950 system with flowing nitrogen environment and 1 °C/min ramp rate. For film composition analysis, Rutherford backscattering spectroscopy (RBS) analysis was carried out on sister samples that were deposited on Si substrates using an NEC 3UH Pelletron with a beam current of 20 nA @ 2.3 MeV. X-ray diffraction (XRD) characterization was done on both CIS powders and thin films deposited on Mo-coated glass using a Siemens D5000 X-ray diffractometer with Cu Kα radiation. Scanning electron microscopy (SEM) images were taken using the cross-section of freshly cleaved CIS samples, which were coated with a thin Pd−Au film to prevent electron charging.

The current vs voltage ($I$−$V$) performance of the finished devices was measured under an Oriel solar simulator with Air Mass 1.5G filter. The light source was calibrated to 1 sun using an Oriel reference cell calibrated and certified by NREL. Field $I$−$V$ measurement on a cloudless day was also performed to confirm the measured efficiency of these devices. External quantum efficiency (EQE) data were taken using a Protoflex QE1400 quantum efficiency measurement system with a Si-InGaAs reference cell.

## Results and Discussion

TGA was utilized to investigate the precursor properties during the thermal decomposition process (Figure 2). A CIS precursor in solid form was prepared by drying the precursor solution under an inert atmosphere at room temperature. This solid precursor was then loaded into a Pt pan and heated to 450 °C under a flowing nitrogen environment. The low-temperature weight loss curve (70−120 °C) indicates the loss of weakly coordinated hydrazine species from the system. The high-temperature transition (250 °C-350 °C) represents the loss of excess chalcogen species. At approximately 350 °C, the weight loss starts to cease. The final product was subjected to XRD analysis, confirming that a high quality CIS phase is formed upon heating the precursor to high temperature.

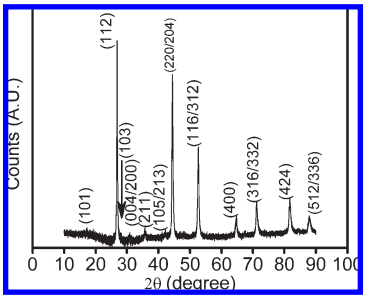


**Figure 3.** Powder X-ray diffraction data of the product obtained after the TGA run shown in Figure 2.

The XRD data is shown in Figure 3, where all major CIS peaks are identified and labeled. The unit-cell parameters, determined by fitting the diffraction pattern, are $a = b =$ 5.754 Å, $c$ = 11.56 Å, $V$ = 382.7 Å$^3$. Comparing to published CIS lattice parameters: $a = b$ = 5.784 Å, $c$ = 11.616 Å, $V$ = 388.6 Å$^3$,[26] the smaller values of lattice constants obtained for this $CuIn(Se,S)_2$ precursor may be caused by the partial substitution of Se with S, which has a smaller atom size.

To tune the bandgap of the hydrazine solution-deposited CIS films and optimize the photon conversion efficiency, we tried to incorporate different amount of S into the final film. Three different types of solutions were used for this purpose. Type I solution was prepared by mixing Cu precursor solution with the "$In_2Se_3$" precursor solution and some amount of Se solution. Type II solution was prepared by mixing Cu solution with the "$In_2(Se,S)_3$" precursor solution (No extra Se or S was added). Type III solution was formed on the basis of type II solution, but with an extra amount of S solution added. Figure 4 shows the XRD results of the CIS (112) and (220/204) peaks of three CIS films deposited using type I, II, and III precursors. It can be seen that the peaks shift to larger $2\theta$ values by increasing the amount of S in the precursor solution. Smaller $d$-spacing indicates that more S (with smaller atom size than Se) was incorporated into the film. RBS analysis was carried out on sister samples (Table 1), confirming that using type II solution significantly increases the amount of S incorporated in the final film compared to using type I solution. However, type III solution does not have a significant impact on further increasing the S content in the final film. By increasing the amount of S in the final film, the bandgap of the CIS system will be enlarged and this can increase the open circuit voltage of the device. This bandgap change can also be seen in the EQE analysis on finished devices, reflected by the shifting of the cut off wavelength (see discussion of EQE data below).

As a polycrystalline material, the grain structure of the CIS film is an important factor that can affect device performance.[27] Although it is believed that sodium diffused from the soda-lime glass substrate can passivate grain boundaries, fine grains with excess grain boundaries

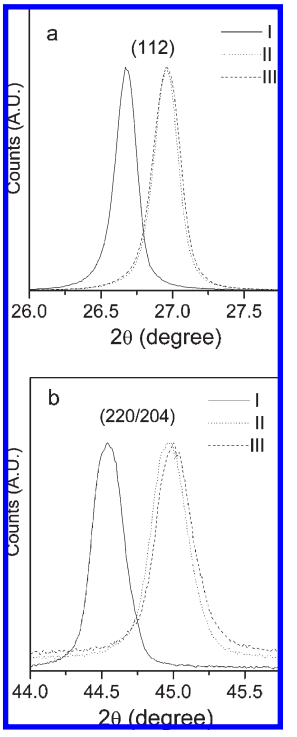


**Figure 4.** XRD data of (a) CIS (112) and (b) CIS (220/204) peaks of films deposited on Mo-coated glass substrates with three different types of precursor solutions (type I, II and III), showing peaks shift to larger $2\theta$ values by increasing the amount of S in the precursor solution. Reflection intensities have been normalized to facilitate comparison between samples.

**Table 1. RBS Results of Film Composition of Three CIS Films Deposited from type I, II, and III Precursor Solutions**

| sample | [Cu] at % | [In] at % | [Se] at % | [S] at % |
|---|---|---|---|---|
| I | 21.1 ± 0.5 | 26.4 ± 0.5 | 47.4 ± 0.5 | 5.1 ± 0.5 |
| II | 22.2 ± 0.5 | 26.4 ± 0.5 | 37.6 ± 0.5 | 13.8 ± 0.5 |
| III | 21.9 ± 0.5 | 26.3 ± 0.5 | 37.3 ± 0.5 | 14.5 ± 0.5 |

can lead to serious recombination and cause a reduction in the current that can be collected. Cross-section SEM images of CIS thin films deposited using this hydrazine approach were taken and two examples are shown in Figure 5. Figure 5a is the grain structure of a CIS film deposited using type I solution and Figure 5b shows the cross-section image of a CIS film with more S deposited using type III solution. As stoichiometry could also affect the grain structure,[20] both films were maintained at a Cu poor composition with Cu to In atomic ratio less than 1. It can be seen that for either case, fairly large grains can be achieved using this hydrazine solution approach.

Finally, complete CIS devices were fabricated following the procedures described previously for CIGS devices.[17−19] Figure 6a shows the AM 1.5G $I-V$ characteristics of two CIS devices with absorbers deposited using two different types of precursor solutions. Sample A is a CIS film deposited with type I precursor solution, with approximately 5% S as measured by RBS. Sample B is a CIS film with ~15% S obtained by using the type III precursor. From the $I-V$ properties of these two devices, it can be seen that by increasing the amount of S incorporated in the film, the open circuit voltage ($V_{oc}$) increases from ~0.43 V to ~0.55 V, whereas at the same time the short circuit current

(26) Stanbery, B. J. *Crit. Rev. Solid State Mater. Sci.* **2002**, *27*(2), 73.
(27) Contreras, M. A.; Romero, M. J.; Noufi, R. *Thin Solid Films* **2006**, *511−512*, 51.

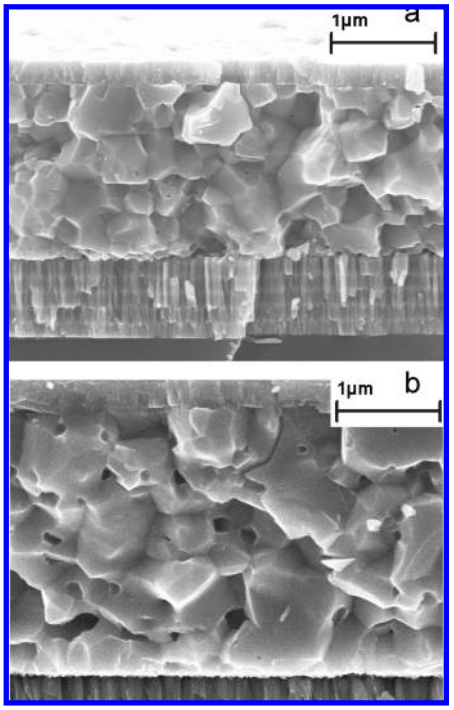


**Figure 5.** SEM cross-section images of two CIS devices: (a) CIS device deposited with type I precursor solution; (b) CIS device deposited with type III precursor (the top layers with small column-shaped grains are CdS/ZnO/ITO).

density ($J_{sc}$) drops from ~37 mA/cm$^2$ to ~30 mA/cm$^2$. Increased $V_{oc}$ is expected because of the larger bandgap obtained by increasing the amount of S in Sample B. The $J_{sc}$ loss is also related to the bandgap change and it can be seen by the shifting of the photon cutoff edge toward shorter wavelength in the EQE measurement results (Figure 6b). The power conversion efficiency $\eta$ increased from 10.7 to 12.2% as a result of the increased bandgap. This is comparable to reported highest efficiency for CIGS deposited using a hydrazine approach [28].

The short wavelength part (below ~500 nm) of the EQE spectrum (Figure 6b) indicates that the absorption from the CdS/ZnO/ITO top layers is similar between these two devices. The longer wavelength region shows that sample A has slightly better photon generated carrier collection than sample B. This indicates the $J_{sc}$ and efficiencies of samples deposited using type III precursor may still have room to improve by optimizing current collection. At the same time, sample A has a longer cut off wavelength that extends to ~1250 nm, whereas sample B's photon response stopped at approximately 1150 nm. The estimated bandgaps of sample A and sample B are approximately 1.08 and 1.15 eV, respectively. Sample A's bandgap is higher than the literature reported value for CIS devices,[3] which may be caused by the small amount of S existing in the CIS film. Sample B's cutoff wavelength is slightly shorter than those reported for very high

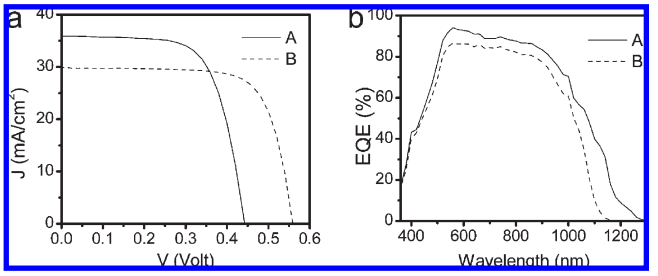


**Figure 6.** (a) $I-V$ and (b) EQE characteristics of two CIS devices A and B. Device A has an absorber deposited with type I precursor solution and the important $I-V$ parameters are $V_{oc}$ = 0.44 V, $J_{sc}$ = 35.9 mA/cm$^2$, FF = 67.5%, and $\eta$ = 10.7%; Device B has an absorber deposited with type III precursor solution and the important $I-V$ parameters are $V_{oc}$ = 0.55 V, $J_{sc}$ = 29.8 mA/cm$^2$, FF = 73.0%, and $\eta$ = 12.2%. The detailed major element compositions of the device A and B absorber layers, as determined by RBS, are device A, Cu(21.1 ± 0.5%), In(26.4 ± 0.5%), Se(47.4 ± 0.5%), S(5.1 ± 0.5%); device B, Cu(24.1 ± 0.5%), In(25.0 ± 0.5%), Se(35.1 ± 0.5%), S(15.8 ± 0.5%).

efficiency CIGS devices with graded band structure.[29,30] Fine tuning the bandgap and/or introducing bandgap grading may help further improve the power conversion efficiency of these hydrazine solution-processed CIS devices and further advance the efficiency table for solution-based techniques.[31]

An integration of the EQE data over the range of wavelengths was carried out based on the ASMT G-173 reference solar spectral irradiance. The resulting theoretical $J_{sc}$ values are 35.7 and 31.6 mA/cm$^2$ for samples A and B, respectively. These values are in reasonable good agreement with the measured $J_{sc}$ values.

## Conclusions

$CuIn(Se,S)_2$ films exhibiting good crystallinity and grain size were successfully deposited using a new solution-based technique in which absorber layer deposition involves precursors dissolved in hydrazine. High power conversion efficiencies, approaching values for devices based on more cost-intensive vacuum-grown CIS as well as previously reported hydrazine-deposited CIGS, were achieved on devices fabricated using these solution processed absorbers. Comparing to hydrazine based CIGS precursors, the CIS precursors are simpler as they do not contain Ga. The process of dissolving into the solution is fast and easy for fewer elements. Yet these precursors maintain the capability to adjust the bandgap of deposited films by changing the amount of S in the precursor solution. The ability to fabricate high-efficiency CIS solar cells further demonstrates the flexibility of the hydrazine-based approach for depositing metal chalcopyrite-based absorber layers and provides further evidence that this approach may offer a low-cost, high-efficiency route to thin-film PV device fabrication.

**Acknowledgment.** The authors thank R. Ferlita for technical support with the preparation of the Ni/Al grid and A. Prabhakar for pre-cleaning the glass substrates. We also thank R. Noufi at National Renewable Energy Lab for providing the shadow mask design used for this study.

(28) Mitzi, D. B. *Adv. Mater.* **2009**, *21*, 3141.
(29) Ramanathan, K.; Contreras, M. A.; Perkins, C. L.; Asher, S.; Hasoon, F. S.; Keane, J.; Young, D.; Romero, M.; Metzger, W.; Noufi, R.; Ward, J.; Duda, A. *Prog. Photovoltaics* **2003**, *11*, 225.
(30) Contreras, M. A.; Ramanathan, K.; AbuShama, J.; Hasoon, F.; Young, D. L.; Egaas, B.; Noufi, R. *Prog. Photovoltaics* **2005**, *13*, 209.
(31) Hibberd, C. J.; Chassaing, E.; Liu, W.; Mitzi, D. B.; Lincot, D.; Tiwari, A. N. *Prog. Photovoltaics* **2009**, in press (DOI: 10.1002/pip.914).